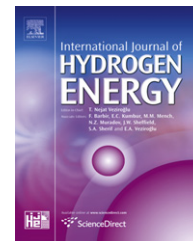


Available at www.sciencedirect.comjournal homepage: www.elsevier.com/locate/he

Modeling and analysis of miniaturized methanol reformer for fuel cell powered mobile applications

Vinay K. Vadlamudi, Srinivas Palanki*

Department of Chemical & Biomolecular Engineering, University of South Alabama, 307 University Blvd N., Mobile, AL 36688-0002, USA

ARTICLE INFO

Article history:

Received 28 May 2010

Received in revised form

30 November 2010

Accepted 14 December 2010

Available online 21 January 2011

Keywords:

Methanol reforming

Reactor design

Hydrogen production

ABSTRACT

In this paper a miniaturized packed bed reactor is analyzed, in which autothermal reforming of methanol occurs to produce sufficient hydrogen for generating 100 W of power. Mass balance equations are developed for each species in the reactor and an energy balance is developed for modeling non-isothermal operation. The pressure drop is modeled via the Ergun equation. Simulations are conducted in MATLAB to determine the effect of process parameters (e.g. steam to methanol ratio, inlet pressure, inlet temperature) on the production of hydrogen. It is shown that the pressure drop is negligible. Simulation results are compared with experimental results from the literature and it shown that there is excellent agreement between the simulation results and experimental results. Process conditions that lead to the generation of sufficient hydrogen for generating 100 W of power are developed. Copyright © 2010, Hydrogen Energy Publications, LLC. Published by Elsevier Ltd. All rights reserved.

1. Introduction

Currently, there is a lot of interest in developing power sources in the 10–100 W range for portable power applications [1,2]. One promising approach involves the use of a reformer that produces hydrogen from a hydrocarbon source, coupled with a fuel cell stack that utilizes the hydrogen to produce power. Such a device can be used to power radios, computers, electronic displays and small unmanned air vehicles [3,4].

There are a variety of commonly available hydrocarbons such as methane, methanol, propane, butane, gasoline, diesel that can be used reforming reactants to produce hydrogen. Among these hydrocarbons, methanol is an attractive choice because it is sulfur-free, offers high hydrogen-to-carbon ratio, high energy density (5600 Wh/kg), and is readily available [5]. Pattekar and Kothare [6] fabricated a radial-flow micro-packed-bed reactor via deep reactive ion etching that utilizes methanol to generate sufficient hydrogen for a 20 W power application. Kundu et al. [1] developed a serpentine patterned micro-reformer that

converts methanol to hydrogen via steam reforming. Shah and Besser [7] developed an integrated silicon microreactor-based methanol steam reformer that produces sufficient hydrogen for 0.38 W of power. Sohn et al. [8] developed a plate-type integrated fuel processor-PEM fuel cell where methanol is reformed to produce up to 150 W of power. Mu et al. [9] fabricated a miniature reformer that utilizes methanol to produce sufficient hydrogen to generate 100 W of power in a fuel cell stack. While there is considerable literature on fabrication of micro reformers that demonstrate the feasibility of utilizing methanol to produce hydrogen for micro and small-scale applications, there are few papers in modeling and analysis of these reactors, which is necessary for optimizing performance. For instance, Telotte et al. [10] developed a simple mathematical model for an isothermal radial-flow methanol reformer for an unmanned air vehicular application that produced 24 W and 72 W of net power by operating at two different points in the polarization curve.

In this paper, an autothermal reformer is designed in a tubular geometry of the type fabricated by Mu et al. [9].

* Corresponding author.

E-mail address: spalanki@usouthal.edu (S. Palanki).

Fundamental principles of reaction engineering, fluid mechanics and heat transfer are utilized to develop this model. The effect of steam to methanol ratio, inlet pressure

Kinetic expressions for reactions 1–3 were developed by Peppley et al. [11,12] and corrected in Peppley [13] and are shown below:

$$r_1 = \frac{k_R K_{\text{CH}_3\text{O}(1)}^* \left(\frac{P_{\text{CH}_3\text{OH}}}{P_{\text{H}_2}^{0.5}} \right) \left(1 - \frac{P_{\text{H}_2}^3 P_{\text{CO}_2}}{K_R P_{\text{CH}_3\text{OH}} P_{\text{H}_2\text{O}}} \right) C_{\text{S}_1}^T C_{\text{S}_{1a}}^T S_C \rho_b}{\left(1 + K_{\text{CH}_3\text{O}(1)}^* \left(\frac{P_{\text{CH}_3\text{OH}}}{P_{\text{H}_2}^{0.5}} \right) + K_{\text{HCOO}(1)}^* P_{\text{CO}_2} P_{\text{H}_2}^{0.5} + K_{\text{OH}(1)}^* \left(\frac{P_{\text{H}_2\text{O}}}{P_{\text{H}_2}^{0.5}} \right) \right) \left(1 + K_{\text{H}(1a)}^{0.5} P_{\text{H}_2}^{0.5} \right)} \quad (5)$$

and inlet temperature on the amount of hydrogen produced is studied. It is shown that there is excellent agreement between the model predictions and experimental results available in the literature. This model is then used to determine the necessary size for operation at the lower end of the feasible range of temperature and pressure.

$$r_2 = \frac{k_D K_{\text{CH}_3\text{O}(2)}^* \left(\frac{P_{\text{CH}_3\text{OH}}}{P_{\text{H}_2}^{0.5}} \right) \left(1 - \frac{P_{\text{H}_2}^2 P_{\text{CO}}}{K_D P_{\text{CH}_3\text{OH}}} \right) C_{\text{S}_2}^T C_{\text{S}_{2a}}^T S_C \rho_b}{\left(1 + K_{\text{CH}_3\text{O}(2)}^* \left(\frac{P_{\text{CH}_3\text{OH}}}{P_{\text{H}_2}^{0.5}} \right) + K_{\text{OH}(2)}^* \left(\frac{P_{\text{H}_2\text{O}}}{P_{\text{H}_2}^{0.5}} \right) \right) \left(1 + K_{\text{H}(2a)}^{0.5} P_{\text{H}_2}^{0.5} \right)} \quad (6)$$

$$r_3 = \frac{k_W K_{\text{OH}(1)}^* \left(\frac{P_{\text{CO}} P_{\text{H}_2\text{O}}}{P_{\text{H}_2}^{0.5}} \right) \left(1 - \frac{P_{\text{H}_2} P_{\text{CO}_2}}{K_W P_{\text{CO}} P_{\text{H}_2\text{O}}} \right) (C_{\text{S}_1}^T)^2 S_C \rho_b}{\left(1 + K_{\text{CH}_3\text{O}(1)}^* \left(\frac{P_{\text{CH}_3\text{OH}}}{P_{\text{H}_2}^{0.5}} \right) + K_{\text{HCOO}(1)}^* P_{\text{CO}_2} P_{\text{H}_2}^{0.5} + K_{\text{OH}(1)}^* \left(\frac{P_{\text{H}_2\text{O}}}{P_{\text{H}_2}^{0.5}} \right) \right)^2} \quad (7)$$

2. System description

Mu et al. [9] fabricated a miniature reformer that utilizes methanol to produce hydrogen and demonstrated that this device has the capability to produce 100 W of power. While this device provides valuable information on feasibility of the concept of miniature reformers for portable power applications, no analysis was done to study the effect of temperature, pressure, oxygen to methanol ratio and steam to methanol ratio on the production of hydrogen. In this paper we develop a mathematical model for this reactor and do a systematic analysis of the effect of operating parameters on system performance.

A schematic of the process under consideration is shown in Fig. 1. The reformer is a packed bed reactor similar to the one fabricated by Mu et al. [9]. The reactor is packed with Cu/ZnO/Al₂O₃ catalyst particles. Methanol and steam enter the reactor where steam reforming reactions occur to produce hydrogen. In addition, methanol is also oxidized in the reactor. There is a jacket around the reactor where methanol is combusted to provide additional heat to the reformer. The resulting hydrogen and carbon dioxide mixture is sent to a fuel cell where an electrochemical reaction occurs to generate power.

where r_1 , r_2 , and r_3 are rates of formation of CO₂, CO and CO₂ in reactions 1, 2 and 3 respectively and P_i is the partial pressure of species i where $i = \text{CH}_3\text{OH}$, H_2O , CO_2 , H_2 , CO , O_2 . These expressions were developed by considering surface mechanism for the main reforming reactions on Cu/ZnO/Al₂O₃ catalyst particles. This model was validated by comparing with experimental observations over a wide range of temperatures and pressures and it was observed that the model predictions were in good agreement with experimental observations [13,14]. Given this experimental validation, this high-fidelity model can be used with a high degree of confidence for designing the miniaturized reformer under consideration in this paper.

The reactions and kinetics for methanol oxidative reforming are obtained from Reitz et al. [15]:

$$r_4 = K_{\text{OX}} \frac{P_{\text{CH}_3\text{OH}}^{0.18} P_{\text{O}_2}^{0.18}}{P_{\text{H}_2\text{O}}^{0.14}} \quad (8)$$

The reformer is modeled as a jacketed packed bed reactor. The steady-state model equations for each species are given by the following mole-balance equations [16]:

$$\frac{d F_{\text{CH}_3\text{OH}}}{d z} = (-r_1 - r_2) A_c \quad (9)$$

$$\frac{d F_{\text{H}_2\text{O}}}{d z} = (-r_1 - r_3) A_c \quad (10)$$

$$\frac{d F_{\text{CO}_2}}{d z} = (r_1 + r_3) A_c \quad (11)$$

$$\frac{d F_{\text{H}_2}}{d z} = (3r_1 + 2r_2 + r_3) A_c \quad (12)$$

$$\frac{d F_{\text{CO}}}{d z} = (r_2 - r_3) A_c \quad (13)$$

where $F_{\text{CH}_3\text{OH}}$, $F_{\text{H}_2\text{O}}$, F_{CO_2} , F_{H_2} , F_{CO} are the molar flow rates of methanol, steam, carbon dioxide, hydrogen, and carbon monoxide respectively and z is the axial dimension of the reactor. The term, A_c , represents the area of cross section of the reactor.

3. Design equations

The following reactions take place in the reformer:

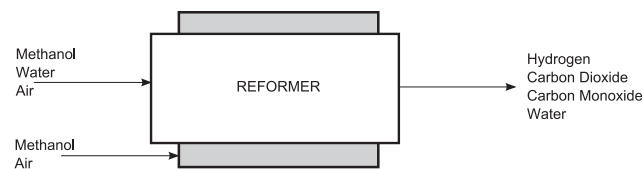


Fig. 1 – Schematic of reformer.

The pressure drop in the packed-bed reactor is modeled via the Ergun Equation as follows [16]:

$$\frac{dP}{dz} = -\frac{G}{\rho D_p} \left(\frac{1-\phi}{\phi^3} \right) \left[\frac{150(1-\phi)\mu}{D_p} + 1.75G \right] \quad (14)$$

where P is the reactor pressure, ϕ is the void fraction, D_p is the diameter of the catalyst particle in the reformer, μ is the viscosity of the gas mixture, ρ is the gas mixture density and G is the superficial mass velocity.

The Ergun equation requires the computation of the gas mixture density, ρ , as well as the gas mixture viscosity, μ , as a function of reactor length. The mixture density is estimated by computing the molar average density of the reacting gas mixture and Wilke's method [17] is utilized to estimate the gas mixture viscosity at each integration step.

A steady state energy balance on the reformer leads to the following equation [16]:

$$\frac{dT}{dz} = \frac{(Ua\Delta T + \sum r_i \Delta H_{r_i}) A_c}{\sum F_j C_{p_j}} \quad (15)$$

where T is the reformer temperature, ΔH_{r_i} is the heat of reaction for reaction r_i , U is the overall heat transfer coefficient between the jacket and the reactor, a is the ratio of the heat transfer area and the reactor volume, ΔT is the temperature difference between the jacket and the reactor at a length z , and C_{p_j} is the specific heat of species j . Methanol combustion occurs in the jacket and so the jacket temperature (~ 1600 K) is significantly greater than the reactor temperature (~ 800 K). Since the reactor is relatively small in length (< 10 cm), it is assumed that the jacket temperature is constant and a separate energy balance for the jacket is not required.

The overall coefficient, U , is constructed from the individual coefficients and the resistance of the tube wall. The overall heat transfer coefficient is calculated by the following equation [18]:

$$U = \frac{1}{\frac{1}{h_i} \frac{D_o}{D_i} + \frac{x_w}{k_m} \frac{D_o}{\left(\ln \frac{D_o}{D_i} \right)} + \frac{1}{h_o}} \quad (16)$$

where D_o is the outer diameter of the tubular reactor, D_i is the inner diameter of the tubular reactor, h_o is the individual heat transfer coefficient at the annulus side of the reactor, h_i is the individual heat transfer coefficient for packed bed reactor side, x_w is the reactor wall thickness and k_m is the thermal conductivity of the reactor wall. The Sieder–Tate equation is used to estimate the individual heat transfer coefficient on the annulus side [18]:

$$h_o = J_H \frac{k_m}{D_o} \left(\frac{C_p \mu_m}{k_m} \right)^{\frac{1}{3}} \quad (17)$$

where J_H is the Colburn j factor, C_p is the average specific heat and μ_m is the mixture viscosity. To predict the rate of heat transfer on the reactor side for different particle and tube sizes, gas flow rates, and gas properties, the coefficient h_i is to account for the resistance in the region very near the wall and for the resistance in the rest of the packed bed. This coefficient is estimated from the following empirical equation, which was determined by subtracting the calculated bed resistance from the measured overall resistance [19]:

$$h_i = \left(0.4 Re_p^{\frac{1}{2}} + 0.2 Re_p^{\frac{2}{3}} \right) Pr^{0.4} \frac{1-\phi}{\phi} \frac{k_{m_i}}{D_p} \quad (18)$$

where Re_p is the Reynold's number for the packed bed reactor, Pr is the Prandtl number, ϕ is the void fraction and k_{m_i} is the average thermal conductivity of the gas mixture.

The reaction rates r_1 , r_2 , r_3 and r_4 are functions of the partial pressure of the various species involved in reactions 1–4. The partial pressures were written in terms of molar flow rates as follows by assuming that the species follow ideal gas behavior:

Table 1 – Kinetic parameters.

Kinetic parameter	Value
k_R	$7.4 \times 10^{14} \exp(-102800/RT) \text{m}^2/\text{mol.s}$
k_D	$3.8 \times 10^{20} \exp(-170000/RT) \text{m}^2/\text{mol.s}$
k_W	$5.9 \times 10^{13} \exp(-87600/RT) \text{m}^2/\text{mol.s}$
K_R	$10^{(1.4142 \times 10^{-13} T^5 - 4.2864 \times 10^{-10} T^4 + 5.3993 \times 10^{-7} T^3 - 3.6385 \times 10^{-4} T^2 + 1.4096 \times 10^{-1} T - 2.0258 \times 10^1)}$
K_D	$10^{(2.9463 \times 10^{-13} T^5 - 8.8919 \times 10^{-10} T^4 + 11.1130 \times 10^{-6} T^3 - 7.4160 \times 10^{-4} T^2 + 2.7969 \times 10^{-1} T - 4.4944 \times 10^1)}$
K_W	$10^{(-1.4936 \times 10^{-13} T^5 + 4.5026 \times 10^{-10} T^4 - 5.6216 \times 10^{-7} T^3 + 3.7206 \times 10^{-4} T^2 - 1.3726 \times 10^{-1} T + 2.4537 \times 10^1)}$
$K_{\text{CH}_3\text{O}(1)}^*$	$\exp(41.8/R - (-20000/(RT))) \text{bar}^{-0.5}$
$K_{\text{CH}_3\text{O}(2)}^*$	$\exp(30/R - (-20000/(RT))) \text{bar}^{-1}$
$K_{\text{HCOO}(1)}^*$	$\exp(-179200/(RT)) \text{bar}^{-1.5}$
$K_{\text{OH}(1)}^*$	$\exp(-44.5/R - (-20000/(RT))) \text{bar}^{-1.5}$
$K_{\text{OH}(2)}^*$	$\exp(30/R - (-20000/(RT))) \text{bar}^{-1}$
$K_{\text{H}(1a)}$	$\exp(-100.8/R - (-50000/(RT))) \text{bar}^{-1}$
$K_{\text{H}(2a)}$	$\exp(-46.2/R - (-50000/(RT))) \text{bar}^{-1}$
$C_{\text{S}1}^{\text{I}}$	$7.5 \times 10^{-6} \text{mol/m}^2$
$C_{\text{S}1a}^{\text{I}}$	$1.5 \times 10^{-5} \text{mol/m}^2$
$C_{\text{S}2}^{\text{I}}$	$7.5 \times 10^{-6} \text{mol/m}^2$
$C_{\text{S}2a}^{\text{I}}$	$1.5 \times 10^{-5} \text{mol/m}^2$

Table 2 – Process parameters.

Process parameter	Value
Catalyst particle diameter, D_p	0.005 m
Catalyst density, ρ_b	1300 kg/m ³
Specific surface area, S_c	102,000 m ² /kg
Void fraction, ϕ	0.38
Reactor length, h	0.07 m
Reactor inner diameter, D_i	0.035 m
Reactor outer diameter, D_o	0.042 m
Reactor wall thickness, x_w	0.0035 m
Reactor wall thermal conductivity, k_m	16.258 W/m/k
Average thermal conductivity of gases in reactor, k_{m_i}	0.071 W/m/k

$$P_j = \frac{F_j}{\sum F_j} P \quad (19)$$

where $j = \text{CH}_3\text{OH}, \text{H}_2\text{O}, \text{CO}_2, \text{H}_2, \text{CO}, \text{O}_2$.

The relation between hydrogen flow rate, current, and the number of cells is given by Larminie and Dicks [20]:

$$I = \frac{2F\varepsilon F_{\text{H}_2}}{n} \quad (20)$$

where I is the current, F is Faraday's constant, F_{H_2} is the molar flow rate of hydrogen entering the fuel cell stack, ε is an efficiency factor and n is the number of cells in the fuel cell stack.

The desired power generated by the fuel cell stack is computed from:

$$P = VI n \quad (21)$$

where P is the power and V is the voltage.

4. Results and discussion

The design equations described by Eq. (9)–(15) were integrated numerically in MATLAB [21] using the stiff ordinary differential equations routine *ode15s*. The kinetic parameters are given in Table 1, process parameters are given in Table 2, specific heats are given in Table 3 and heats of reaction are given in Table 4. The steam reforming reactions are endothermic and it is necessary to provide additional heat to keep the reformer in a temperature range where it is possible to get close to 100%

Table 4 – Heats of reaction.

$\Delta H_{r1} = 4.95 \times 10^4 + (C_{p_{\text{CO}_2}} + 3C_{p_{\text{H}_2}} - C_{p_{\text{CH}_3\text{OH}}} - C_{p_{\text{H}_2\text{O}}})(T - 298) \text{ J/mol}$
$\Delta H_{r2} = 9.07 \times 10^4 + (C_{p_{\text{CO}}} + 2C_{p_{\text{H}_2}} - C_{p_{\text{CH}_3\text{OH}}})(T - 298) \text{ J/mol}$
$\Delta H_{r3} = -4.12 \times 10^4 + (C_{p_{\text{CO}_2}} + C_{p_{\text{H}_2}} - C_{p_{\text{H}_2\text{O}}} - C_{p_{\text{CO}}})(T - 298) \text{ J/mol}$
$\Delta H_{r4} = -6.752 \times 10^5 + (2C_{p_{\text{H}_2\text{O}}} + C_{p_{\text{CO}_2}} - C_{p_{\text{CH}_3\text{OH}}} - 1.5C_{p_{\text{O}_2}})(T - 298) \text{ J/mol}$

conversion. The required heat can be provided in two ways: (1) oxidation of methanol in reforming chamber and (2) combustion of methanol in jacket. To design the heat transfer jacket, the inner pipe diameter, annulus diameter, inlet pressure, inlet reactor temperature and inlet jacket temperature are used to calculate the individual heat transfer coefficients for the inside and outside of the pipe (Eq. (17) and (18)). The overall coefficient is constructed from the individual coefficients and the resistance of the tube wall using Eq. (16). The overall heat transfer coefficient is a function of temperature and flow rate. For $T_i = 773 \text{ K}$, and a methanol flow rate of $4 \times 10^{-4} \text{ mol/s}$, the overall heat transfer coefficient was found to be 9.4 J/m^2 . A variation of 10% in the flow rate and temperatures resulted in a change of less than 1% in the value of the heat transfer coefficient. For this reason, a constant value of 9.4 J/m^2 was used in the simulations.

Mu et al. [9] fabricated a mini reformer that has the same dimensions as the reformer considered in this research for autothermal reforming of methanol to produce hydrogen. To compare the theoretical results from this research with experimental results, it is necessary to first estimate the effectiveness factor for the reactor system. However, details of the particle size, constriction factor and tortuosity were not provided in Mu et al. [9]. To get an order of estimate of the effectiveness factor, the methanol kinetics represented by Eq. (1) was linearized and the other reactions (Eq. (2)–(4)) were neglected. The Thiele modulus and effectiveness factor were calculated by assuming a constriction factor of 0.5, tortuosity of 10 and particle porosity of 0.2 [16]. For these values, the effectiveness factor was found to be equal to 1.5×10^{-3} . When the values of constriction factor, tortuosity and particle porosity were varied by $\pm 50\%$, the effectiveness factor was of the order of 10^{-3} . The value of effectiveness factor was further refined by using a single experimental value of Mu et al. [9]. When the reformer was run experimentally at an inlet temperature of 773 K, inlet pressure of 400 kPa, oxygen to

Table 3 – Specific heat of gases.

Species	Specific heat (J/mol/K)				
H_2	$C_{p_{\text{H}_2}} = a_1 + b_1 \left(\frac{T}{100}\right) + c_1 \left(\frac{T}{100}\right)^2 + d_1 \left(\frac{T}{100}\right)^3 + e_1 \left(\frac{1000}{T}\right)^2$				
H_2O	$C_{p_{\text{H}_2\text{O}}} = a_2 + b_2 \left(\frac{T}{100}\right) + c_2 \left(\frac{T}{100}\right)^2 + d_2 \left(\frac{T}{100}\right)^3 + e_2 \left(\frac{1000}{T}\right)^2$				
CO_2	$C_{p_{\text{CO}_2}} = a_3 + b_3 \left(\frac{T}{100}\right) + c_3 \left(\frac{T}{100}\right)^2 + d_3 \left(\frac{T}{100}\right)^3 + e_3 \left(\frac{1000}{T}\right)^2$				
CO	$C_{p_{\text{CO}}} = a_4 + b_4 \left(\frac{T}{100}\right) + c_4 \left(\frac{T}{100}\right)^2 + d_4 \left(\frac{T}{100}\right)^3 + e_4 \left(\frac{1000}{T}\right)^2$				
O_2	$C_{p_{\text{O}_2}} = a_5 + b_5 \left(\frac{T}{100}\right) + c_5 \left(\frac{T}{100}\right)^2 + d_5 \left(\frac{T}{100}\right)^3 + e_5 \left(\frac{1000}{T}\right)^2$				
CH_3OH	$C_{p_{\text{CH}_3\text{OH}}} = 63.4$				
Where					
$a_1 = 33.066178$	$a_2 = 30.92000$	$a_3 = 24.99735$	$a_4 = 25.56759$	$a_5 = 29.65900$	
$b_1 = -11.363417$	$b_2 = 6.832514$	$b_3 = 55.18696$	$b_4 = 6.096130$	$b_5 = 6.137261$	
$c_1 = 11.432816$	$c_2 = 6.7934356$	$c_3 = -33.69137$	$c_4 = 4.054656$	$c_5 = -1.186521$	
$d_1 = -2.772874$	$d_2 = -2.534480$	$d_3 = 7.948387$	$d_4 = -2.671301$	$d_5 = 0.095780$	
$e_1 = -0.158558$	$e_2 = 0.0821398$	$e_3 = -0.136638$	$e_4 = 0.131021$	$e_5 = -0.219663$	

methanol ratio of 0.21 and steam to methanol ratio of 1.4, a conversion of 86.6% was obtained. We ran simulations under these initial conditions and determined that for an effectiveness factor value of 1.5×10^{-3} , the conversion obtained was 86.85%. This value of effectiveness factor also agrees with the literature [22] where it is stated that the effectiveness factor for this system typically varies between 10^{-4} – 10^{-3} . This value of effectiveness factor was used in all remaining simulations. One must be cautious in interpreting the effectiveness factor calculations since the assumption of first order kinetics is questionable given the large nonlinearities in the reaction terms. Furthermore, the assumption of isothermal conditions is clearly violated. The use of a value of effectiveness factor of 1.5×10^{-3} in our simulations should be treated more as a fitted parameter or a ball-park estimate rather than as a parameter fundamental to the model with a sound physical significance.

The effect of inlet temperature, inlet pressure and steam to methanol ratio on the production of hydrogen was analyzed by running simulations as follows:

- Inlet steam to methanol ratio range: 1–1.4
- Inlet pressure range: 200–400 kPa
- Inlet temperature range: 773–833 K

The oxygen to methanol ratio was kept at 0.21 to avoid unsafe operation [9]. The above process conditions are chosen because the reaction kinetics developed in the literature is valid in this range. Simulations were conducted at various process conditions to determine a set of conditions where at least 8×10^{-4} mol/s of hydrogen is produced. It will be shown later that this flow rate is sufficient to produce 100 W of power.

Fig. 2 shows the comparison between experimental results of Mu et al. [9] and the simulation results of the model developed here when the steam to methanol ratio is varied from 1.0 to 1.4 at an inlet temperature of 773 K and inlet pressure of 400 kPa. It is observed that there is excellent agreement between theoretical predictions and experimental results. This indicates that the simulation results can be used for rapid determination of suitable reactor conditions for optimized production of hydrogen.

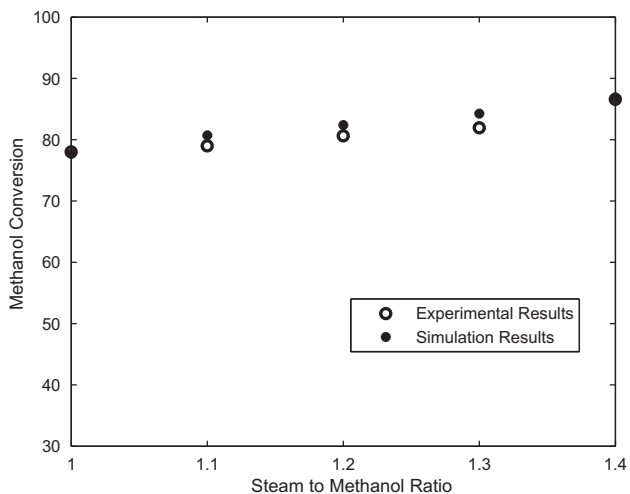


Fig. 2 – Comparison between experimental results and theoretical predictions for methanol conversion.

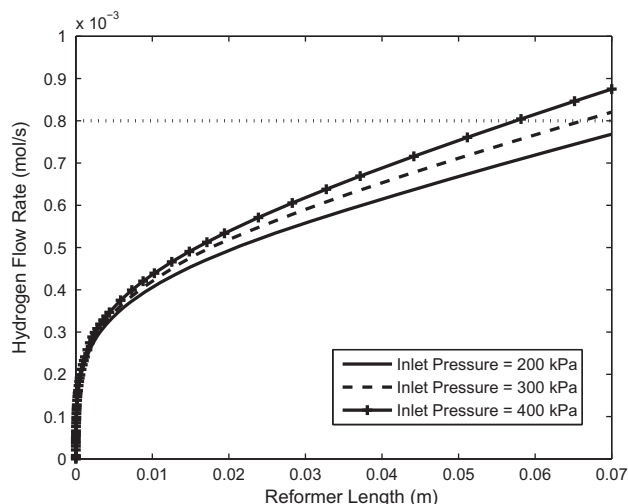


Fig. 3 – Effect of varying inlet pressure on hydrogen flow rate.

Fig. 3 shows the effect of inlet pressure on hydrogen flow rate out of the reformer when the inlet temperature is 803 K and the steam to methanol ratio is 1.2. It is observed that as the inlet pressure increases, the outlet flow rate of hydrogen increases. When the inlet pressure is 200 kPa, there is no sufficient hydrogen generated to produce 100 W of power. Fig. 4 shows the pressure along the length of the reactor at an inlet temperature of 803 K, inlet pressure of 200–400 kPa, and steam to methanol ratio of 1.2. It is observed there is negligible pressure drop along the length of the reactor. There is an increase in the number of moles along the length of the reactor, which tends to increase the pressure; however there is pressure drop due to flow of gases in the packed bed. The pressure profiles in Fig. 4 indicate that these two competing effects balance out leading to negligible pressure drop. In these simulations, we used a particle diameter of 0.005 m. The paper by Mu et al. [9] did not indicate the particle diameter used in their experiments. The use of a smaller diameter will lead to an increase in pressure drop.

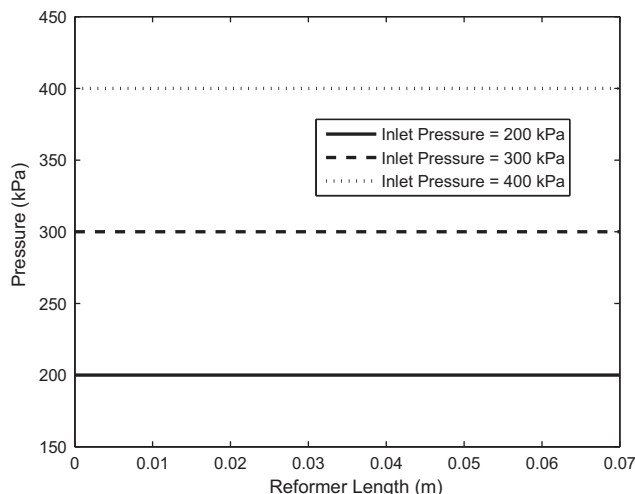


Fig. 4 – Pressure as a function of reactor length.

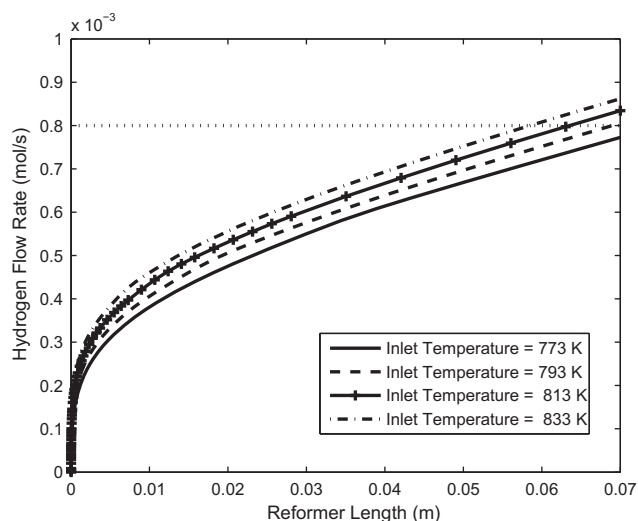


Fig. 5 – Effect of varying inlet temperature on hydrogen flow rate.

Fig. 5 shows the effect of changing inlet temperature between 773 K and 833 K on hydrogen flow rate out of the reformer at an inlet pressure of 300 kPa and a steam to methanol ratio of 1.2. It is observed that as the inlet temperature is increased, the outlet flow rate of hydrogen coming out of the reactor increases due to higher reforming rates. While increasing temperature, increases the amount of hydrogen produced, this comes at the cost of increased heat duty. For practical applications, it is necessary to use the lowest possible temperature, the lowest possible pressure above atmospheric, and the lowest possible steam to methanol ratio. The effect of increasing the length of reactor from 0.07 m to 0.10 m on hydrogen production was studied. Due to increase in residence time of reactants, it is possible to get higher conversion. Fig. 6 shows the results of this simulation study where the inlet pressure is kept at 200 kPa, the inlet temperature is kept at 773 K, the inlet oxygen to methanol ratio is

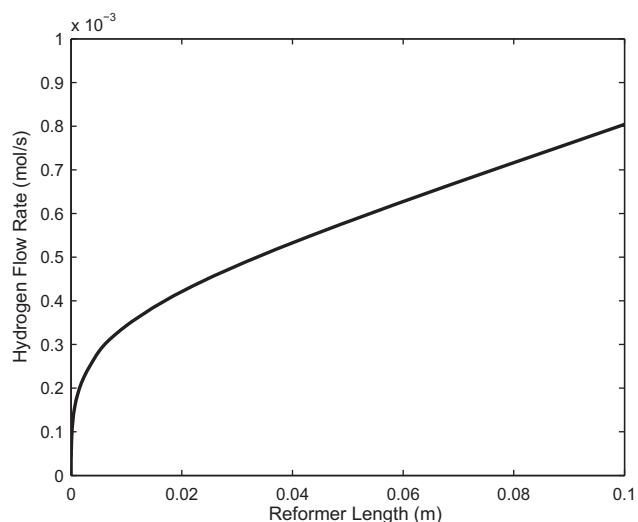


Fig. 6 – Effect of increasing reformer length on hydrogen flow rate.

Table 5 – Fuel cell parameters.

Number of cells, n	25
Area of cross section of each cell, A	20.25 cm ²
Efficiency factor, ε	0.95
Faraday's constant, F	96,487 Cmol ⁻¹
Inlet flow rate of Hydrogen, F_{H_2}	8×10^{-4} mol/s

kept at 0.21 and the inlet steam to methanol ratio is kept at 1.0. It is observed that for this longer reactor, the hydrogen flow rate is 8×10^{-4} mol/s.

The hydrogen coming out of the reformer has carbon monoxide as an unwanted side product that can result in detrimental operation on certain types of fuel cells (e.g. PEM fuel cells). In this case, one has to scrub the reformer exit gas of the carbon monoxide as detailed in Alagharu et al. [23]. A suitable fuel cell stack was developed to verify that a hydrogen flow rate is 8×10^{-4} mol/s could, indeed, produce 100 W of power. The procedure developed in Alagharu et al. [23] was used to design a fuel cell stack. The parameters of the stack are given in Table 5. The polarization curve shown in Fig. 7 was utilized to model the relation between voltage and power density, which was developed from experimental data at 60 °C by Chang et al. [24]. It is observed that a stack of 25 cells results in a current of 5.86 A and a voltage of 0.68 V. Using Eq. (21), a total power of 100 W is produced. The above simulations were done for a fixed flow rate of methanol to produce sufficient hydrogen for generating 100 W of power. Due to the polarization effect in the fuel cell, changing the flow rate of methanol has a nonlinear effect on the power generated since increasing hydrogen flow rate results in an increase in current density but a decrease in voltage. Temperature also affects the polarization curve characteristics significantly. The effect of flow rate and temperature on the total power produced in a fuel cell are discussed in more detail in Kolavennu et al. [25].

The model developed in this paper assumes that the system is at steady state. It is possible to use a formal optimization procedure as illustrated in Choi and Stenger [26] for determining the optimal operating conditions for this system. For dynamic

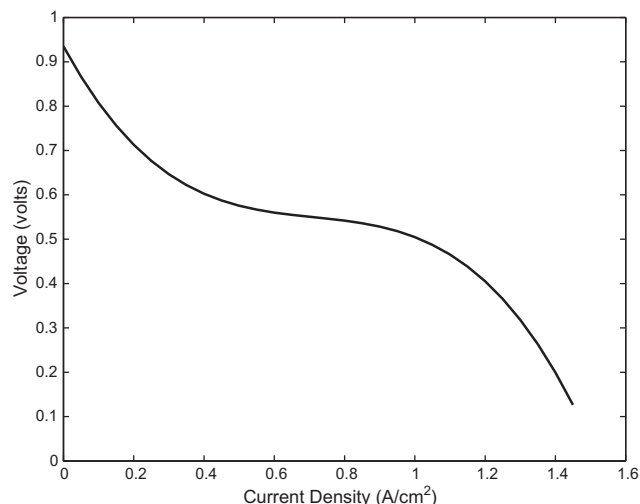


Fig. 7 – Polarization curve.

analysis and controller design, it is necessary to develop a dynamic model for the reformer-fuel cell system and the reader is referred to Kolavennu et al. [27] for a description of how an adaptive controller can be designed for tracking time-varying power profiles in a reformer-fuel cell system.

5. Conclusions

In this paper, an autothermal reformer was analyzed to generate 100 W of power for portable device applications. In this process both the steam reforming reactions and oxidation reactions occur in the reformer. Furthermore, methanol is combusted in the jacket to provide additional heat to the reformer. The reformer dimensions are taken from an experimental system designed by Mu et al. [9]. The reformer operates non-isothermally in an inlet temperature range of 773 K–853 K, inlet pressure range of 200–400 kPa, and steam to methanol ratio of 1.0–1.4 to obtain sufficient hydrogen to generate 100 W of power. It is observed that pressure drop is negligible throughout the reactor volume. The simulation results are in excellent agreement with the conversion obtained experimentally by Mu et al. [9]. It is shown that to operate the reactor at the lower end of the range of parameters considered, it is necessary to increase the reactor length from 0.07 m to 0.10 m.

REFERENCES

- [1] Kundu A, Jang JH, Gil JH, Jung CR, Lee HR, Kim SH, et al. Micro-fuel cells-current development and applications. *J Power Sources* 2007;170:67–78.
- [2] Service RF. Shrinking fuel cells promise power in your pocket. *Science* 2002;296:1222.
- [3] National Research Council. Meeting the energy needs of future warriors, <http://www.nap.edu/catalog/11065.html>; 2004.
- [4] Unmanned Aircraft systems Roadmap 2005–2030, Office of the Secretary of Defense, U.S. DOD; 2005.
- [5] deWild PJ, Verhaak MJFM. Catalytic production of hydrogen from methanol. *Catal Today* 2000;60:310.
- [6] Pattekar AV, Kothare MV. A radial microfluidic fuel processor. *J Power Sources* 2005;147:116–27.
- [7] Shah K, Besser RS. Understanding thermal integration issues and heat loss pathways in a planar microscale fuel processor: demonstration of an integrated silicon microreactor-based methanol steam reformer. *Chem Eng J* 2008;135S:S46–56.
- [8] Sohn JM, Byun YC, Cho JY, Choe J, Song KH. Development of the integrated methanol fuel processor using micro-channel patterned devices and its performance for steam reforming of methanol. *Int J Hydrogen Energy* 2007;32:5103–8.
- [9] Mu X, Pan L, Liu N, Zhang C, Li S, Sun G, et al. Autothermal reforming of methanol in a mini-reactor for a miniature fuel cell. *Int J Hydrogen Energy* 2007;32:3327–34.
- [10] Telotte JC, Kern J, Palanki S. Miniaturized methanol reformer for fuel cell powered mobile applications. *Int J Chem Reactor Eng* 2008;6:A64.
- [11] Peppley BA, Amphlett JC, Kearns LM, Mann RF. Methanol-steam reforming on Cu/ZnO/Al₂O₃ catalysts. Part 1. The reaction network. *Appl Catal A* 1999;179:21–9.
- [12] Peppley BA, Amphlett JC, Kearns LM, Mann RF. Methanol-steam reforming on Cu/ZnO/Al₂O₃ catalysts. Part 2. A comprehensive kinetic model. *Appl Catal A* 1999;179:31–49.
- [13] Peppley BA. Personal communication, www.southalabama.edu/engineering/chemical/faculty/palanki/research/res/peppley06.pdf; 2006.
- [14] Asprey SP, Wojciechowski BW, Peppley BA. Kinetic studies using temperature-scanning: the steam-reforming of methanol. *Appl Catal A* 1999;179:51–70.
- [15] Reitz TL, Ahmed S, Krumpelt M, Kumar R, Kung HH. Characterization of Cu/ZnO under oxidizing conditions for the oxidative methanol reforming reaction. *J Mol Catal A Chem* 2000;162:275–85.
- [16] Fogler HS. *Elements of chemical reactor engineering*. Upper Saddle River: Prentice-Hall; 2006.
- [17] Poling BE, Prausnitz JM, O'Connell JP. *The properties of gases and liquids*. 5th ed. McGraw-Hill; 2001.
- [18] McCabe WL, Smith JC, Harriot P. *Unit operations of chemical engineering*. 6th ed. NY: McGraw-Hill; 2001.
- [19] Tosun I. *Modeling in transport phenomena*. 2nd ed. U.K.: Elsevier B.V. 2007.
- [20] Larminie J, Dicks A. *Fuel cell systems*. New York: Wiley; 2000.
- [21] Matlab. Natick, MA 01760: The Mathworks; 2007.
- [22] Chen Z, Yan Y, Elnashaie SSEH. Modeling and optimization of a novel membrane reformer for higher hydrocarbons. *AIChE J* 2003;49:1250–65.
- [23] Alagharu V, Palanki S, West KN. Analysis of ammonia decomposition reactor to generate hydrogen for fuel cell applications. *J Power Sources* 2010;195:829–33.
- [24] Chang H, Kim JR, Cho JH, Kim HK, Choi KH. Materials and processes for small fuel cells. *Solid State Ionics* 2002;148:601–6.
- [25] Kolavennu P, Telotte JC, Palanki S. Design of a fuel cell power system for automotive applications. *Int J Chem Reactor Eng* 2006;4. Article A19.
- [26] Choi Y, Stenger HG. Kinetics, simulation and optimization of methanol steam reformer for fuel cell applications. *J Power Sources* 2005;142:81–91.
- [27] Kolavennu P, Palanki S, Cartes DA, Telotte JC. Adaptive controller for tracking power profile in a fuel cell powered automobile. *J Process Control* 2008;18:558–67.